Numerical Simulation of Separated Flows in Three-Dimensional Industrial Geometries: A Case Study

Gary J. Brown

Alcoa of Australia Limited, Kwinana, Western Australia

ABSTRACT

The commercial computational fluid dynamics (CFD) package CFX4.1 is used to predict the swirling gas flow inside an air heater used in the alumina calcining process. Comparison of the numerical predictions with flow visualisation performed using a 1:35.6 scale water model of the system reveals that the numerical model fails to predict a vortex in the heater inlet caused by flow separation on a radiused bend. Subsequent modeling shows that prediction of the vortex at 1:35.6 scale can only be achieved using a low Reynolds number k-ε model in conjunction with a very fine wall mesh in order to resolve the wall boundary layer. Use of the low Reynolds number k-ε model for the full-scale system is impractical and hence a high Reynolds number k-ε model using log-layer wall functions is used in conjunction with a wall mesh with the first wall node located just outside the wall surface roughness. With this configuration the numerical model is able to predict the presence of the vortex in the full-scale system, not detected in the early results. This result highlights the necessity for local grid refinement at walls in regions where flow separation may occur and illustrates the potential for error in the use of coarse mesh results. The work also illustrates the complexity of creating fine wall meshes inside three-dimensional models of real process equipment when using hexahedral structured meshes.

NOMENCLATURE

B	Log-law constant
C_μ	Turbulence model constant (0.09)
k	Turbulence kinetic energy
u	Velocity component parallel to wall
u*	Friction velocity
u^+	Non-dimensional velocity
y	Wall distance
y^+	Non-dimensional wall distance
ε	Turbulence dissipation
ε_w	Roughness height
ε_w^+	Non-dimensional roughness
κ	Von Karman's constant (0.41)
ν	Fluid kinematic viscosity
ρ	Fluid density
τ_w	Wall shear stress

1. INTRODUCTION

During 1995 Fuel and Combustion Technology Ltd. (FCT) undertook a physical modeling study for Alcoa to determine the performance of an air heater used in the alumina calcining process. The geometry of the air heater system is shown in figure 1. A tangential inlet and exit create a swirling flow in the cylindrical air heater body. Combustion is achieved through the use of a natural gas burner located in the roof of the air heater.

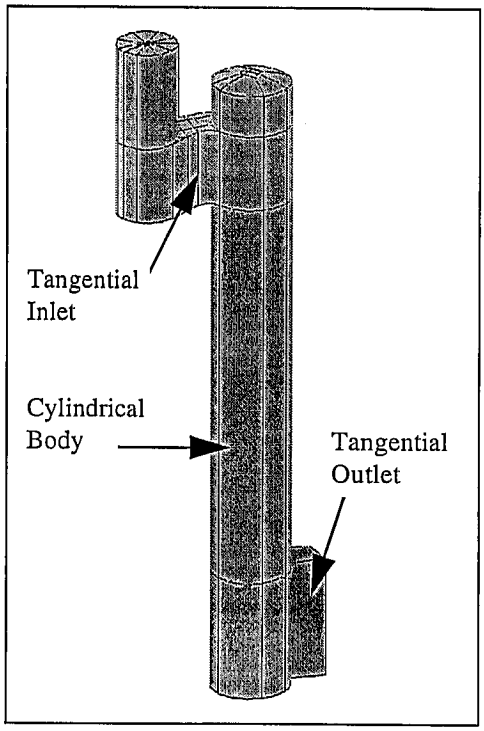

Figure 1 Air heater geometry

As part of this study, flow visualisation for the air heater was undertaken. The information obtained from this study provided an ideal opportunity for the validation of numerical models that were being developed at that time to investigate similar flows. As such, a numerical modeling study was initiated to predict the full-scale air heater flow and to compare these predictions with the results of the small-scale physical modeling study.

2. BACKGROUND THEORY

2.1 The Turbulent Boundary Layer

In fully developed turbulent flow over a smooth wall the near-wall flow can be divided into three regions: an inner wall layer where viscous shear dominates, an outer layer where turbulent shear dominates, and an overlap layer where both types of shear are important. The outer layer is not of specific interest here and so will not be discussed in detail. However the description of the inner and overlap layers are important.

The inner viscous sub-layer is described by the *law of the wall* deduced by Prandtl;

$$u^+ = \frac{u}{u^*} = F\left(\frac{yu^*}{\nu}\right) \qquad (1)$$

where u* is termed the friction velocity and is defined in terms of the wall shear stress;

$$u^* = \left(\frac{\tau_w}{\rho}\right)^{1/2} \qquad (2)$$

In the overlap layer it is found that a reasonable transition between the inner and outer wall profiles can be achieved if the velocity varies logarithmically with distance from the wall, y;

$$\frac{u}{u^*} = \frac{1}{\kappa}\ln\frac{yu^*}{\nu} + B \qquad (3)$$

where κ is Von Karman's constant ($\approx$0.41) and B$\approx$5.0. Equation (3) is referred to as the logarithmic-overlap law or *log-law*.

In the range $0<y^+<5$ the law of the wall follows the linear viscous relation;

$$u^+ = \frac{u}{u^*} = \frac{yu^*}{\nu} = y^+ \qquad (4)$$

with the wall velocity profile then changing and merging with the log-law at $y^+\approx30$. The log-law is then found to give a good representation of the flow out to $y^+\approx1000$. The actual intersection of equations (4) and (3) occurs at $y^+\approx11$. These concepts are illustrated in figure 2.

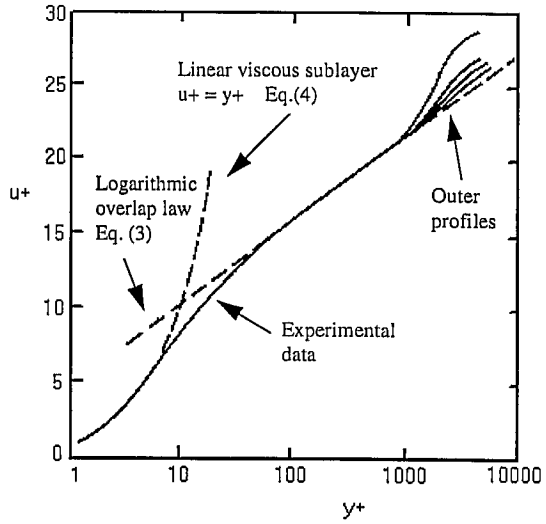

Figure 2 Turbulent wall velocity profile

Surface roughness has a significant impact on the near-wall flow. The logarithmic profile still holds but is shifted to the right by an amount approximately equal to ln ε_w^+, where;

$$\varepsilon_w^+ = \frac{\varepsilon_w u^*}{\nu} \qquad (5)$$

As the surface roughness is increased the viscous sub-layer begins to disappear and is eventually totally broken up, with the result that for $\varepsilon_w^+>70$ friction becomes independent of viscosity and hence Reynolds number (Schetz, 1993). In this fully rough regime the modified log-law becomes;

$$\frac{u}{u^*} = \frac{1}{\kappa}\ln\frac{y}{\varepsilon_w} + 8.5 \qquad (6)$$

2.2 Wall Functions

In numerical modeling the task of capturing the near-wall behaviour of the flow is complicated by several factors. Firstly, it would be necessary to use a very fine mesh to resolve the large gradients in the flow variables and, secondly, viscous effects at the walls need to be incorporated into the turbulence model equations.

Some commercial CFD codes do provide turbulence models modified in this way, generally referred to as low Reynolds number models. The CFX4.1 code (AEA Technology, 1995) used in this study provides a low Reynolds number variant of the k-ε model (Launder and Sharma, 1974). Because these models rely upon an adequate resolution of the laminar viscous sublayer it is necessary to use a very fine wall mesh with several cells in the range $0<y^+<5$.

The requirements for very fine wall meshes and modified turbulence models can be avoided through the use of suitable *wall-functions* which connect the wall shear stress to the dependent variables at the near-wall grid node, located outside the viscous sub-layer. These wall-functions, however, rely upon the assumption of an equilibrium boundary layer.

Using the standard k-ε turbulence model as an example, the most common approach in commercial CFD codes is to calculate the turbulence kinetic energy, k, in the near-wall control volume and to then use this to calculate the wall shear stress through the relation;

$$\tau_w = \rho C_\mu^{1/2} k \qquad (7)$$

The velocity component parallel to the wall is then obtained through use of the log-law velocity profile (equations (3) and (6)) and the turbulence dissipation through the relation;

$$\varepsilon = \frac{C_\mu^{3/4} k^{3/2}}{\kappa y} \qquad (8)$$

It is generally recommended that the first wall node be located in the range $30<y^+<100$ for greatest accuracy when using wall functions based on the log-law profile.

3. PHYSICAL MODELING

The physical modeling study was undertaken using a 1:35.6 scale perspex model of the full-scale geometry. Water was used as the working fluid and the flow patterns were visualised through the illumination of neutrally buoyant beads introduced to the flow. The Reynolds number in the small-scale system was 21,000, based upon the hydraulic diameter in the air heater inlet, compared to a value of 650,000 in the full-scale system. However, this difference was not expected to affect the validity of the small-scale model because both flows were in the fully turbulent Reynolds number regime.

A schematic interpretation of the observed flow patterns in the air heater inlet is shown in figure 3. Of most significance is that the flow does not follow the contour of the radiused bend in the inlet, but rather separates on the corner and forms a reversed flow region, or stalled vortex.

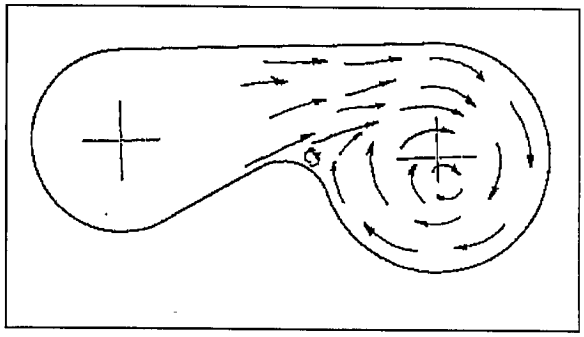

Figure 3 Experimental flow patterns

4. NUMERICAL MODELING

4.1 Initial numerical model

4.1.1 Full-scale air heater system

Initially, a numerical model was developed of the full-scale air heater. The numerical model incorporated the complete geometry investigated in the physical model, shown in figure 1. The numerical model was developed using the commercial code CFX4.1, which utilises a block-structured hexahedral mesh.

The block-structured mesh facility was used in this geometry to overcome several mesh quality problems that can arise with fully structured codes. For example, a multi-block structure was used inside the cylindrical body of the air heater to improve the orthogonality of the mesh, and to align the mesh as much as possible with the swirling flow (figure 4). However, a dependence on hexahedral cells has limitations, especially in areas where the geometry is degenerate. For example, the outer walls of the inlet duct meet the main body of the air heater at pure tangents. This means that, at least on the top and bottom surfaces of the inlet duct, the orthogonality of the mesh is compromised because of the need to fit hexahedral cells into a degenerate wedge-shaped region. This problem is illustrated in figure 5, which shows a magnification of the mesh in the region where the radiused inlet duct intersects the main heater body. It should also be noted that in such regions the cells become

increasingly skewed as the cell size is decreased.

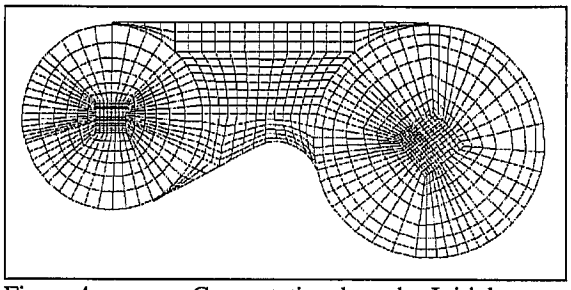

Figure 4 Computational mesh; Initial numerical model of full-scale heater.

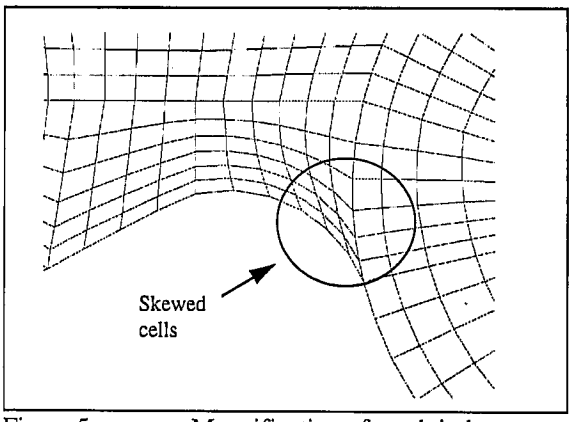

Figure 5 Magnification of mesh in heater inlet.

The complexity of achieving a high quality refined mesh inside the air heater geometry was one of the reasons why the initial numerical model was created with a reasonably coarse mesh. Another factor influencing this decision was that, to be of practical benefit in a production environment, the run-time for the model on a standard UNIX workstation needed to be less than 12 hours (an over-night run). Given that the ultimate goal was to be able to run the model with multiple phases using a Reynolds stress turbulence model, 50,000 cells was seen as a practical limit.

For these reasons, a reasonably coarse mesh was initially created, which consisted of approximately 42,000 cells (figures 4 and 5). Simulations were subsequently performed using this mesh, in conjunction with a differential Reynolds stress turbulence model and second-order convective differencing (Van Leer TVD (Total Variation Diminishing) scheme).

The predicted flow patterns in the air heater inlet are presented in figure 6. Comparison of this figure with the experimental results presented in figure 3 reveals significant differences, in that the numerical model does not predict a separation of the flow from the radiused corner in the heater inlet. This result raised questions about the accuracy of the numerical model, but also created doubts about the physical modeling. The Reynolds number and surface roughness in the full-scale and small-scale systems were significantly different. Were the experimental results actually indicative of the full-scale flow?

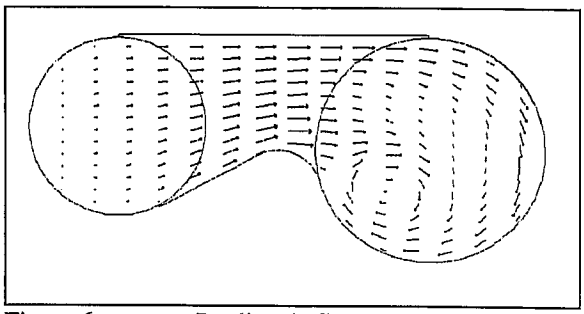

Figure 6 Predicted flow patterns; Initial numerical model of full-scale heater.

In an attempt to resolve these issues it was decided to validate the numerical model by predicting the physical modeling results, and to then use this validated numerical model to predict the full-scale flow. Before this occurred, however, a closer inspection of the full-scale numerical model created doubts about the accuracy of these predictions. Correct prediction of the separated flow, if it existed at the full-scale, would be dependent on adequate resolution of the boundary layer on the radiused bend in the heater inlet. However, the wall y^+ values in this region were found to be in the range $700<y^+<1000$. This is at the upper end of the range of applicability of the log-law, indicating that the wall cells were too large.

4.1.2 Small-scale water model

A numerical model of the 1:35.6 scale water model was developed. The mesh was created to ensure that the wall y^+ values on the radiused bend were in the range $30<y^+<100$, consistent with the requirements for the use of log-law wall functions. Because of the differences in scale and Reynolds numbers between the full-scale and small-scale systems it was possible to meet this y^+ requirement by simply scaling the full-scale mesh to 1:35.6 scale. As such, the computational mesh used was as presented in figures 4 and 5.

Given that the wall cells had been matched to the y^+ requirement for the log-law wall functions, the numerical model was expected to give accurate results. An assumption of smooth walls in the water model was made and simulations were again performed using a differential Reynolds stress turbulence model and second-order convective differencing. However, the numerical model predicted the same flow patterns that had been predicted for the full scale system (figure 6), at variance to the observed experimental results (figure 3).

4.2 Refined numerical model

4.2.1 Small-scale water model

The failure of the numerical model to predict the observed separation on the radiused bend in the physical modeling clearly indicated that the wall boundary layer in this region was not being adequately resolved. An initial attempt was made to reduce the size of the walls cells further, whilst still using log-law wall functions. However, this became impractical because a small reduction in the cell size brought the wall y^+ value to less than 11, the minimum value at which the log-law could reasonably be used. Because the wall cells were too small this also resulted in the calculation of unphysical values for ε in the wall cells and hence convergence difficulties.

Given this problem, and the need to accurately resolve the wall boundary layer, it was decided to proceed with the modeling using the low Reynolds number k-ε model provided in CFX (see section 2.2).

Following some initial testing using a two-dimensional model, a fully three-dimensional model of the small-scale air heater was developed, using a very fine wall mesh (the centre of the wall cells was at approximately $y^+=1$). Because of the large number of computational cells required, it would have been computationally too expensive to create a model of the full geometry show in figure 1. Instead, a three-dimensional model was developed which concentrated just on the inlet region to the air heater (figure 7).

Despite the reduced geometry this model had approximately 53,000 computational cells, compared to the 42,000 cells in the original full geometry. The much increased cell density can been seen by comparing figure 8 below with figure 5 presented earlier for the original numerical model.

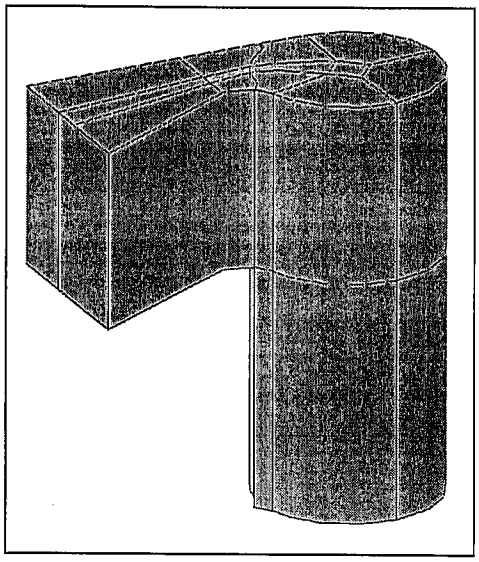

Figure 7 Geometry for refined numerical model.

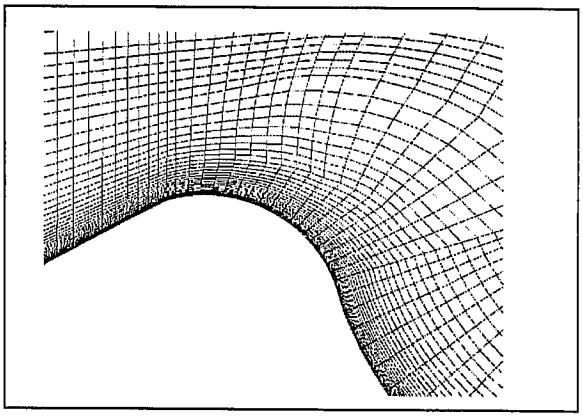

Figure 8 Magnification of mesh in heater inlet. Refined numerical model of small-scale heater.

Creating such a fine wall mesh inside the air heater geometry presented a serious challenge given the hexahedral cell limitation. It was desired to create a high quality mesh on the radiused corner in order to correctly predict the wall boundary layer and, as such, the block structure used in the initial numerical model was unsuitable because it would have resulted in unacceptably skewed cells at the required mesh density (see figure 5).

A block structure was eventually developed which allowed a high quality mesh in the region of the corner and the air heater inlet. The mesh is shown in figure 8 and the underlying block structure in figure 9.

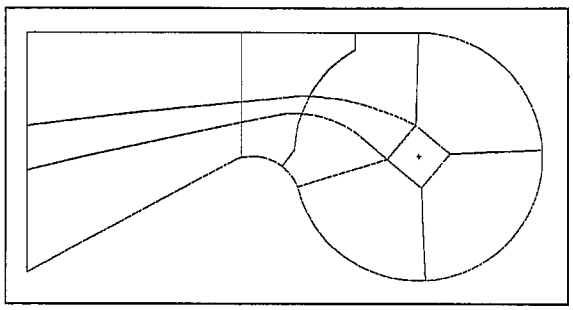

Figure 9 Mesh block structure. Refined numerical model of small-scale heater.

Whilst this block structure gives a high quality mesh in the inlet region it can be seen that when the blocks are extruded to give the main body of the air heater the resulting shape will not be a perfect cylinder. Instead, there will be two square corners on the air heater body. Obviously this is a far from perfect result, but the mesh created in this instance was considered to be satisfactory because it gave the desired quality and resolution in the main area of interest i.e. on the radiused bend.

It should be pointed out that, whilst numerous discussions with other CFD practitioners have revealed other methods of creating the desired inlet mesh density, the author is not currently aware of any technique that could be used in this situation without sacrificing the true geometry in some way.

Simulations were conducted using the refined model, again assuming smooth walls and using second order convective differencing. The predicted flow patterns achieved with the refined numerical model using the low Reynolds number k-ε model are presented in figure 10. This shows that the model was able to predict separation of the flow and the formation of a low velocity reversed flow region on the radiused bend. Comparison of the predicted flow patterns in figure 10 with the physical modeling results in figure 3 shows good qualitative agreement, highlighting the need for accurate resolution of the wall boundary layer in these type of flows.

A magnification of the flow patterns in the reversed flow region on the radiused bend is given in figure 11. This shows that the region actually consists of two counter-rotating vortices, one formed by separation of the inlet flow on the bend and the other formed by separation of the recirculating flow stream inside the air heater.

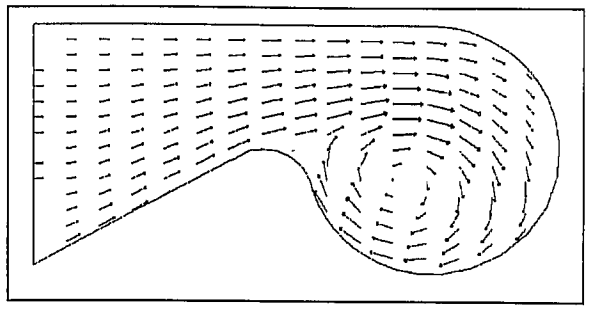

Figure 10 Predicted flow patterns; Refined numerical model of small-scale heater.

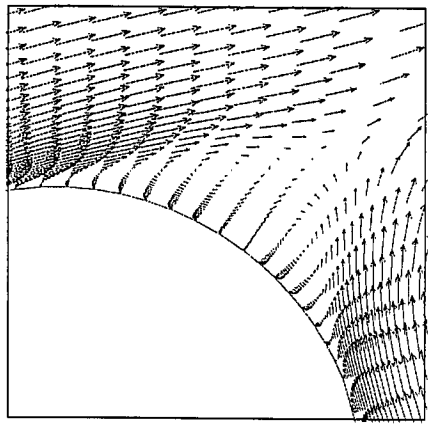

Figure 11 Magnification of flow vectors in separated flow region.

Figure 12 provides a close magnification of the flow next to the wall inside the reversed flow region, showing the resolution of the wall boundary layer through the use of the very fine computational mesh and the low Reynolds number k-ε model.

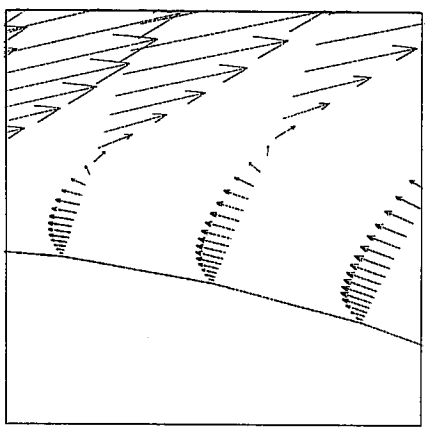

Figure 12 Resolution of the boundary layer shape.

4.2.2 Full-scale air heater system

As discussed in section 4.1.1, the initial differences between the numerical predictions at the full-scale, and the small-scale water model results, raised questions about the

accuracy of both sets of results and about what the full-scale flow really looked like. This lead to the decision to validate the numerical model by predicting the experimental results, and to then use the validated numerical model to predict the full-scale flow.

This type of validation technique is used routinely throughout industry and academia for the prediction of full-scale flows, and in many cases it is a technically sound approach. However, this case illustrates what is one of the grey areas in terms of numerical model validation. The aim of validation is that, having gained agreement with the experimental results, predicting the full-scale flow is then simply a case of changing the geometry and fluid properties in the numerical model to the full-scale and running the model again, without any changes to the numerical schemes employed.

This idealised approach was not possible in this case, and the reason again came back to the treatment of the wall boundary conditions. In the refined numerical model of the small-scale water model the wall boundary layer was resolved using a very fine wall mesh in conjunction with the low Reynolds number k-ε model. In this model, several cells were placed inside the laminar sub-layer, which exists in the region $y^+<5$. Applying the same technique at the full-scale was not possible for several different but connected reasons.

Firstly, the much higher Reynolds number (650,000 vs 21,000 at the small-scale) results in a much thinner boundary layer with respect to the overall geometry. This meant that, in order to fully resolve the boundary layer, an even finer wall mesh would have been required in the full-scale model than had been used in the water-model predictions (figure 8). Such a mesh would have been impractical to construct and would have lead to an extremely large number of cells in the model.

Secondly, the full scale air heater is lined with refractory and has a significant surface roughness, which changes the properties of the wall boundary layer. Using wall shear stress values taken from preliminary simulations it was found that the condition $\varepsilon_w^+>70$ was met at the wall and hence the laminar sub-layer would be completely broken up by the surface roughness. This obviously prevented the use of a technique which relies upon resolving the laminar sub-layer.

The next best approach was to return to the use of log-layer wall functions and, for the best resolution of the boundary layer, to place the centre of the wall cells just outside the wall roughness height. Note that there is also a sound mathematical reason for not making the wall cells smaller than this - equation (6) will predict a negative velocity if the distance to the cell centre from the wall, y, is less than the surface roughness height, ε_w.

This requirement regarding the height of the wall cells resulted in a significantly coarser wall mesh than had been used in the small-scale predictions. An enlargement of the computational mesh used in the inlet region is given in figure 13. Comparison with the refined mesh used for the small-scale simulations (figure 8) shows that the wall mesh is significantly more coarse. However, it should be noted that the computational mesh was still considerably finer than in the original numerical model developed (see figure 5). The y^+ values in the wall cells in the refined model were found to be in the range $30<y^+<300$ (Note that the shift of the log-law due to surface roughness causes an increase in y^+ for a given u^+ (see section 2.1))

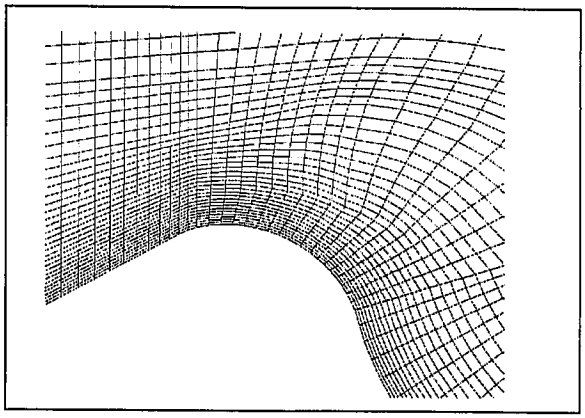

Figure 13 Magnification of mesh in heater inlet. Refined numerical model of full-scale heater.

The overall geometry used was as per the refined small-scale model (figure 7). However, as a result of the larger wall cells the overall number of cells in the model reduced from approximately 53,000 to approximately 38,000.

The predicted flow patterns achieved with this model are shown in figure 14. The flow

patterns are very similar to the predicted (figure 10) and observed (figure 3) flow patterns at the small-scale, which is a very important result for several reasons.

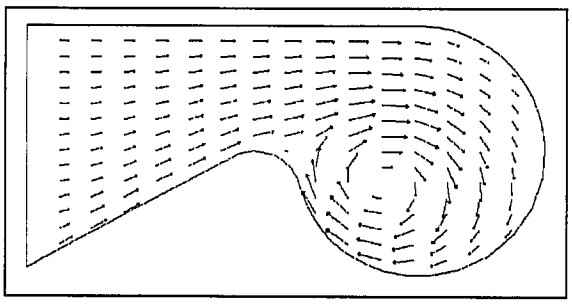

Figure 14 Predicted flow patterns; Refined numerical model of full-scale heater.

Firstly, it confirms that the small-scale water model is representative of the full-scale and, secondly, it illustrates that despite the changes to the numerical model, it is still able to predict the flow separation at the full-scale. This in itself tells us something very interesting about the full-scale and small-scale flows and the numerical techniques required to achieve correct predictions.

At the small-scale the low Reynolds number and smooth walls result in a wall boundary layer of significant height with respect to the overall geometry. As such, it is not satisfactory to make an equilibrium log-layer assumption about the boundary layer shape and instead the true shape of the boundary layer must be resolved, including the laminar sub-layer. At the full-scale the high Reynolds number and significant surface roughness destroy the laminar sub-layer and the log-layer profile (Eq.(6)) provides a closer approximation to the true boundary layer shape over the region of interest. The use of log-layer wall functions is therefore justified and, as discussed above, provides the only practical solution. However, correct prediction of the separated flow still depends upon adequate resolution of the boundary layer. Unfortunately, at the time of writing the author has not been able to complete a grid refinement study to determine how coarse the wall mesh can be made whilst still achieving correct prediction of the separated flow.

5. CONCLUSIONS

This study has highlighted the care that needs to be exercised when attempting numerical simulations of problems which may involve flow separation. For a low Reynolds number flow in a 1:35.6 scale water model of an industrial air heater, it was found that flow patterns observed experimentally could not be predicted through the use of a high Reynolds number turbulence model and log-layer wall functions. Instead, it was necessary to use a low Reynolds number k-ε model in conjunction with a very fine wall mesh in order to resolve the wall boundary layer. For the full-scale flow the use of the standard k-ε turbulence model and log-layer wall functions was found to be adequate, but a fine wall mesh was again required to correctly predict the flow.

The creation of such fine wall meshes inside the complex three-dimensional geometry of the air heater presented a serious challenge given the use of a block-structured hexahedral element code, to the extent that it was found necessary to alter the true geometry in order to achieve a fine wall mesh of sufficient quality. Because of these complexities, many CFD practitioners tend to use models with coarse wall meshes when examining systems with complex geometries. The results of this study should serve as a warning in this regard.

ACKNOWLEDGMENTS

The author wishes to acknowledge the assistance provided throughout this study by Fuel and Combustion Technology Ltd.

REFERENCES

AEA Technology, (1995), CFX4.1 User Guide, AEA Technology, Harwell Laboratory, Oxfordshire, UK.

Launder, B. E. and Sharma, B. T. (1974), Application of the energy dissipation model of turbulence to the calculation of flow near a spinning disc, *Lett. Heat and Mass Transfer 1*, pp 131-138.

Schetz, J.A., (1993), *Boundary Layer Analysis*, Prentice Hall, New Jersey.